Parametric PSF estimation via sparseness maximization in the wavelet domain

Filip Rooms[a], Wilfried Philips[a] and Javier Portilla[b]

[a] Dept. Telecommunication and Information Processing, Ghent university, Belgium, {frooms,philips}@telin.ugent.be

[b] Dept. of Computer Science and Artificial Intelligence, Universidad de Granada, javier@decsai.ugr.es

Keywords: parametric kernel estimation, wavelets, sparseness, image deblurring

ABSTRACT

Image degradation is a frequently encountered problem in different imaging systems, like microscopy, astronomy, digital photography, etc. The degradation is usually modeled as a convolution with a blurring kernel (or Point Spread Function, PSF) followed by noise addition. Based on the combined knowledge about the image degradation and the statistical features of the original images, one is able to compensate at least partially for the degradation using so-called image restoration algorithms and thus retrieve information hidden for the observer. One problem is that often this blurring kernel is unknown, and has to be estimated before actual image restoration can be performed. In this work, we assume that the PSF can be modeled by a function with a single parameter, and we estimate the value of this parameter. As an example of such a single-parametric PSF, we have used a Gaussian. However, the method is generic and can be applied to account for more realistic degradations, like optical defocus, etc.

1. INTRODUCTION

Images represent a snapshot of the state of an object for later investigation, or to use automatic processing on the image. A problem often encountered here is image degradation, i.e., blurring and noise. This degradation often hinders visual interpretation of the images, as well as automatic processing of the images by image analysis software.

Therefore, it is desirable to compensate at least partly for this image degradation. The degradation is modeled as follows:

$$g(x,y) = N\left((h * f)(x,y)\right)$$

where $g(x,y)$ is the observed, degraded image. $f(x,y)$ represents the unknown, ideal image we wish to recover and $h(x,y)$ is the blurring kernel (or Point Spread Function, PSF, i.e, the image of a single ideal point by the imaging system). $N(\cdot)$ represents the noise processes that influence the imaging process. Often, noise is modeled to be additive, and independent of the underlying signal. In that case, we can rewrite the previous equation as:

$$g(x,y) = (h * f)(x,y) + n(x,y)$$

where $n(x,y)$ is the additive noise (in this work we assume i.i.d. Gaussian noise of known variance; when its variance is unknown however, it is relatively easy to estimate [1,2]).

A problem in image restoration is that the blurring kernel $h(x,y)$ is often unknown, or only partially known. In this case, $h(x,y)$ has to be estimated. This estimation can be performed prior to the restoration process (which we will refer to as *blur estimation*), or simultaneously during the restoration process (which we will refer to as *blind deconvolution*). A good review of the latter kind of methods can be found in [3,4]. In this class, there are also a few methods that alternatively estimate the image and the blurring kernel [5–8]. Blind deconvolution algorithms usually are complex, and have a heavy computational load.

Further author information: (Send correspondence to Filip Rooms)
Filip Rooms: E-mail: frooms@telin.UGent.be, Telephone: +32-9-264.34.15

Wavelet Applications in Industrial Processing II, edited by Frédéric Truchetet, Olivier Laligant, Proc. of SPIE Vol. 5607 (SPIE, Bellingham, WA, 2004)
0277-786X/04/$15 doi: 10.1117/12.571539

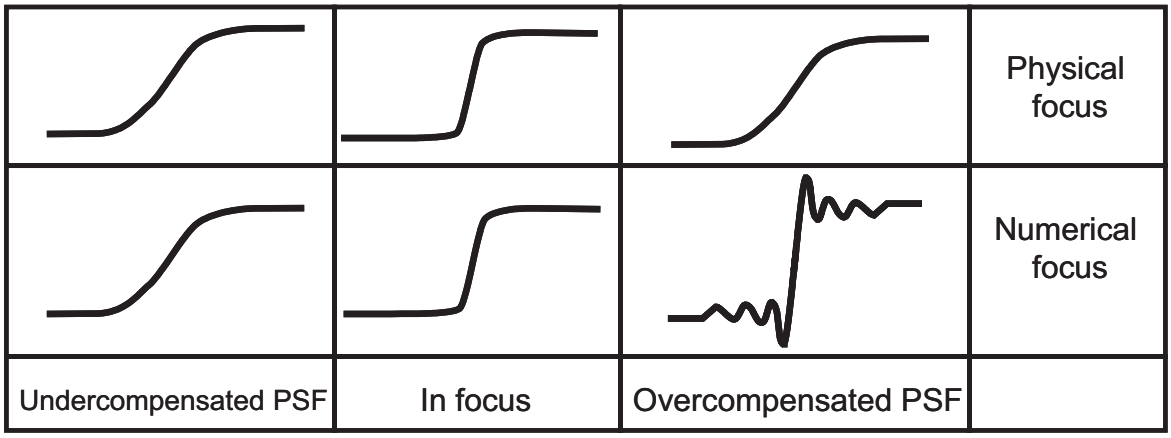

Figure 1. Physical versus numerical focus effect on the cross-section of an edge.

We will now give a summary of common methods for *blur estimation* (loosely inspired on [9], who considered blur estimation for image analysis). A first approach is based on the analysis of the zero patterns in the Fourier spectrum [10–12]. This approach is particularly useful in estimating motion blur and out-of-focus blur, since those produce characteristic zero patterns in the Fourier spectrum. On the other hand, it is not suitable for Gaussian PSF's. Another approach assumes an autoregressive (AR) model for the underlying image, while the blur is modeled by a moving average (MA) process. The blur estimation is then transformed into the estimation of the parameters of the AR-MA model. In [13, 14] a maximum likelihood method is proposed to estimate the blur parameters is proposed. In [15, 16], the estimation of the parameters relies on the method of Generalized Cross-Validation (GCV). Another approach is described in [17], which is in fact not a parametric blur estimation method, but a method to decide which of a set of given blurring kernels is the best for restoration (even if those kernels are not of some parametric form). This method minimizes the spectral difference between the image restored with the different candidate kernels, and the spectrum which should be found when the degraded is restored with the most likely kernel according to a prior model on the spectral distributions of typical images.

Our paper is organized as follows: in section 2, we discuss the principle behind our method. In section 3, we discuss experimental evaluation and comparison of our method. We have chosen [17] to compare our results with because it has some intrinsic similarities with our method. Finally in section 4, we draw some conclusions.

2. OUR METHOD

The approach followed in this work has been to use a standard fast non-blind regularized deconvolution technique (we have used a simple Wiener implementation) to obtain image estimations for a wide range of values of the PSF parameter (the σ_{blur} of an isotropic 2D Gaussian function, in this case). Observing the features of those estimations, we search for a criterion that tells us when the image is "in focus". "In focus" here has a different meaning than in a physical focusing system: in a physical focusing system, it is sufficient to judge when the image reaches maximal sharpness (e.g., has maximal high frequency energy content). However, when applying digital deconvolution, over-correction of the PSF effect in the presence of noise gives raise to overshoot and ringing of the image edges (see Figure 1).

In this paper, we propose a wavelet-based criterion for choosing the optimal PSF parameter. For signals having strong localized discontinuities (such as edges, corners, etc., in images), the wavelet representations are powerful decorrelating tools. On the other hand, in the last decade, it has been widely studied how a mixing linear transformation (the PSF convolution, in our case) increases the mutual information between the mixed elements, and how applying Principal Component Analysis (PCA) to the mixed observations is not enough for recovering the original (unmixed) elements. That can be achieved, under certain conditions, by searching for the inverse linear transform that minimizes the mutual information of the transformed observations (Independent Component

Analysis, ICA). In practice, to achieve strictly that minimization is challenging, so several simpler approximated criteria have been proposed [18–21]. In the case of images, it has been observed that wavelet coefficients are very "sparse" [22–24], that is, the significant features are concentrated in relatively few coefficients (in this work we have used an à trous Haar wavelet, which is the simplest decorrelating multiscale transform). Loosely speaking, in this context a high sparseness of the wavelet coefficients is a sign of relatively low mutual information between them. Or, in other words, by maximizing a measurement of sparseness we decrease the mutual information.

Using the previous background, this work is based on the two following observations:

1. blurring, as a local linear mixing, most often decreases the sparseness of the wavelet subbands;
2. overcompensating for the blur (that is, trying to invert a blur stronger than the actual blur) typically has a similar effect of reducing the sparseness of the wavelet responses.

This effect can be understood by applying a derivative filter (a similar effect to that of the wavelet) to the recovered edge of Figure 1: the response is maximally concentrated when the image is "in focus". As a means to characterize the sparseness we have used the kurtosis of each wavelet subband (e.g., [18, 20, 24]). We have tested empirically that when an image is not degraded, its wavelet subbands have typically maximal kurtosis, compared to the ones obtained with the same image convolved with a slight low-pass filter or its inverse (high-pass). Thus, the wavelet subbands of under- or oversharpened images have typically lower kurtosis values.

We would like to use as a reference the highest frequency subbands that are still relatively noise-free. The reason for preferring the high-frequency subbands instead of the low frequency subbands is that we want to use wavelet subbands as much affected by the image blur as possible. We have found empirically that a good compromise is to choose the subbands around the frequency f_{ref} for which the observed signal power spectral density is 4.5 dB above the noise level (Figure 2). We denote the finest of these two scales by HB and the coarsest by LB; their maximal bandpass frequencies fall respectively at f_{HB} and f_{LB}. Then we checked which values of the PSF parameter maximized the kurtosis in these two neighboring scales after Wiener restoration with this candidate PSF. To calculate the kurtosis for a certain scale, the wavelet subbands with the horizontal and vertical detail coefficients were merged into one vector (the diagonal wavelet subband was discarded):

$$\begin{aligned} \sigma_{max,HB} &= \arg \max_{\sigma_{blur}} \text{kurtosis}(coefficients\ HB\ (Wienerfilter(g(x,y), \sigma_{blur}, \sigma_{noise}))) \\ \sigma_{max,LB} &= \arg \max_{\sigma_{blur}} \text{kurtosis}(coefficients\ LB\ (Wienerfilter(g(x,y), \sigma_{blur}, \sigma_{noise}))) \end{aligned}$$

Then we took a weighted average of these PSF parameter values, giving more weight when f_{ref} is closer to the maximum of the bandpass of a wavelet scale. The difference in frequency d_L is the difference in frequency between f_{LB} and f_{ref}, while d_H is the difference in frequency between f_{HB} and f_{ref},

$$\begin{aligned} d_L &= f_{ref} - f_{LB} \\ d_H &= f_{HB} - f_{ref} \end{aligned}$$

so the weighted average becomes

$$\sigma_{blurest} = \frac{\sigma_{max,LB}\ d_H + \sigma_{max,HB}\ d_L}{f_{HB} - f_{LB}}$$

3. EVALUATION AND COMPARISON

We have evaluated the method using several natural images degraded with different amounts of blur and noise. As mentioned before, we used a simple Wiener implementation to obtain image estimations for each value of the PSF parameter, which we swept through the interval $\sigma_{blur} = 0.4$ to $\sigma_{blur} = 6.0$ with discrete steps of $\Delta\sigma_{blur} = 0.2$. The range of noise values considered in our experiments was $\sigma_{noise} = 0.1$ to $\sigma_{noise} = 10.0$. The method provided satisfactory results for this range of blur and noise levels.

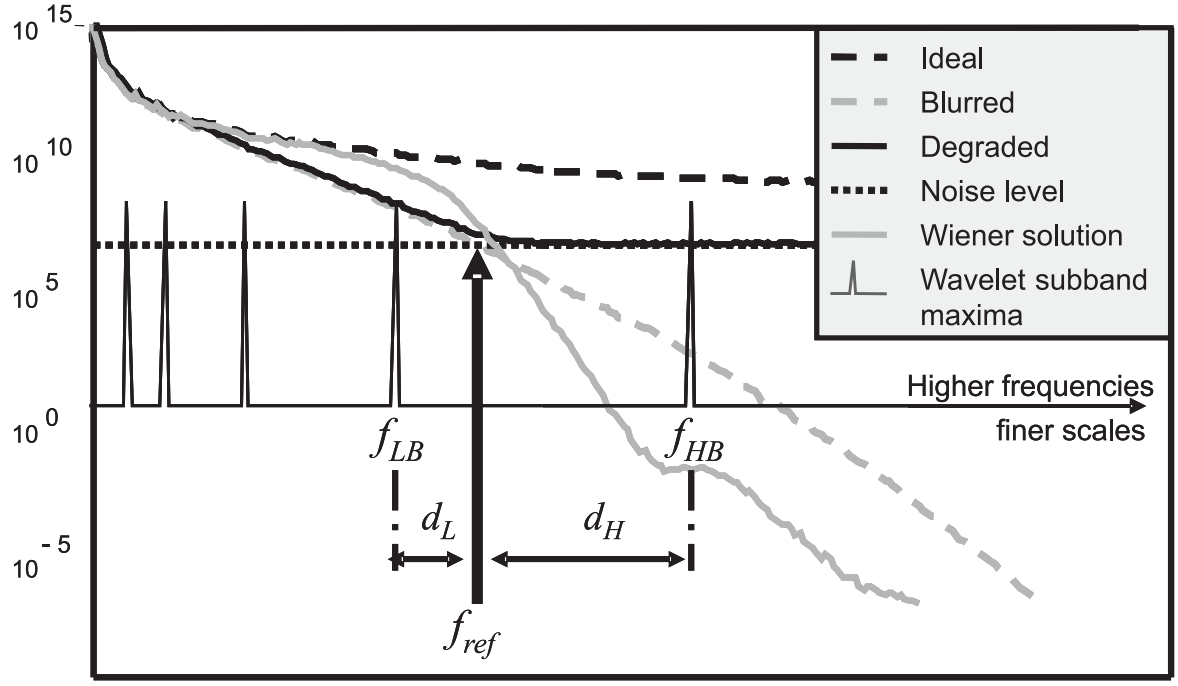

Figure 2. Reference frequency in the Fourier spectrum and choice of wavelet subbands to monitor for sparseness maximization.

As a method for comparison, we implemented Savakis' method [17]. This method determines which PSF from a set of given candidates minimizes the difference between the spectrum of the image restored with the candidate PSF and the spectrum as it is supposed to be after Wiener restoration, under a prior model for the image power spectral density. In other words, this method minimizes the difference between $Q_{R_i}(u,v)$, which is the residual spectrum after Wiener restoration with this $h_i(x,y)$, and $Q_{E_i}(u,v)$, which is the residual spectrum we expect after Wiener restoration with the "right" PSF. Savakis considered amongst others the *Chi square test*:

$$\chi^2 = \sum_{u,v} \frac{|S_E(u,v) - S_{R_i}(u,v)|^2}{S_E(u,v)}$$

where $S_E(u,v)$ and $S_{R_i}(u,v)$ are the respectively normalized spectra $Q_E(u,v)$ and $Q_{R_i}(u,v)$.

In the set of graphs in Figure 3 we show the average estimated blur values obtained for our set of five test images (*Airplane*, *Peppers*, *House*, *Flintstones* and *Lake*). The top row shows the results obtained with Savakis' method, while the bottom row shows the results obtained with our method. The left column shows the results of both methods without any compensation, while the right column shows the results compensated to minimize the overall error. Savakis' method tends to underestimate the blur for all blur and noise levels, which can partially be corrected by adding 0.5 to σ_{blur} (when comparing Figure 3 (a) and (c), the compensated curves are closer to the real values). However, the errors in Savakis' method depend both on the blur and the noise level, and are therefore very difficult to compensate completely. On the other hand, our method tends to overestimate the blur systematically for higher noise levels (the reason why is still not clear, and has to be investigated further). Since we assumed the noise level to be known, we can compensate accordingly. We have hand-optimized the following heuristic expression to compensate for this overestimation:

$$\sigma_{blur,compensated} = \sigma_{blur} + 0.0011\sigma_{noise}^2 - 0.0397\sigma_{noise} - 0.1594$$

Compared to Savakis' method, we have almost completely removed the estimation bias. This is an important advantage, which doesn't translate in a much lower MSE value, however.

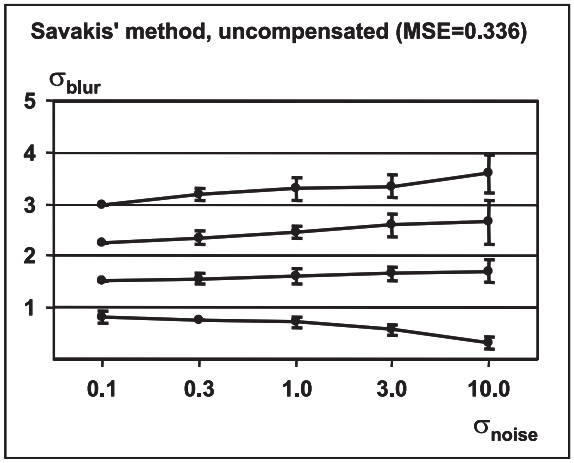

(a) Savakis' method without compensation.

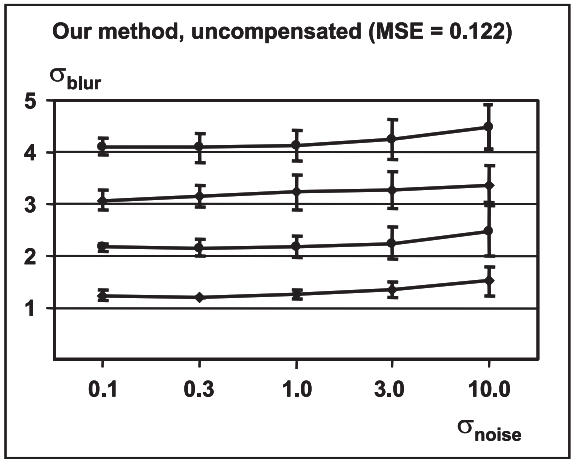

(b) Our method without compensation

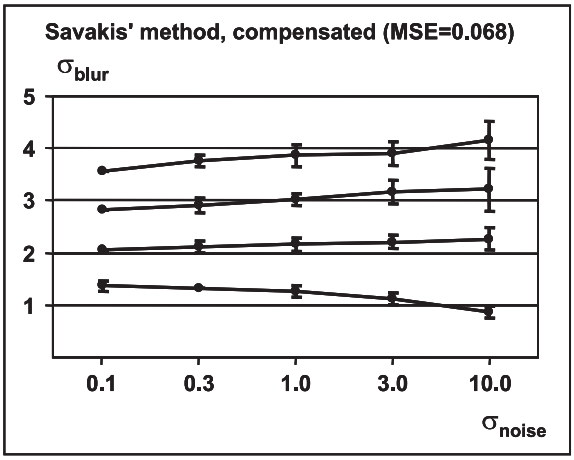

(c) Savakis' method with compensation.

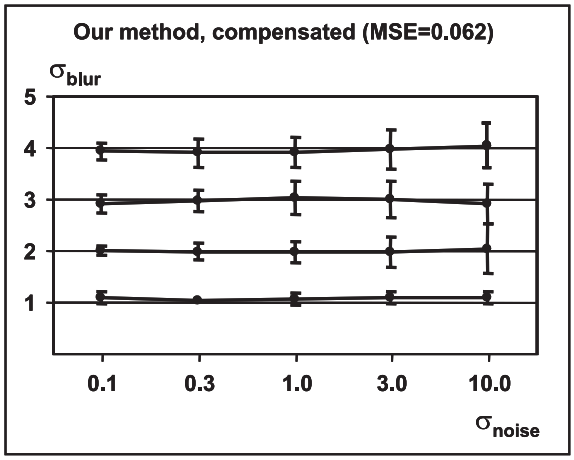

(d) Our method with compensation.

Figure 3. Summaries of blur estimation results for our method and Savakis' method, both uncompensated and compensated. In each graph, a horizontal line represents the estimations for 4 different blur levels for a range of noise levels. The error bars correspond to $(\mu+\sigma, \mu-\sigma)$, with μ the sample mean and σ the sample standard deviation over the test set. In each of the 4 subfigures (a-d), the horizontal curves correspond with $\sigma_{blur,real} = 1$ (bottom curve) to $\sigma_{blur,real} = 4$ (top curve).

To give an example of the robustness of the restoration result for small errors in σ_{blur}, we restored the *Lake*. The real degradation parameters were $\sigma_{blur,real} = 2.0$, $\sigma_{noise} = 10.0$. We restored the degraded image with a Wiener filter using the real σ_{noise}, but swept σ_{blur} between 0.6 and 4.0. This way, we obtained a curve for the PSNR in function of σ_{blur} (Figure 4). It shows a slow rise of the PSNR when σ_{blur} increases towards $\sigma_{blur,real}$. When σ_{blur} is close to $\sigma_{blur,real}$, the PSNR is more or less stable, which means that the restoration result is relatively insensitive for small errors of σ_{blur} in that region. When σ_{blur} is increased even further, the value of the PSNR drops steeply. In Figure 5, we show some restoration results on the *Lake* image using the estimated blur values, for two extreme situations (first: low blur, high noise level; second: high blur, low noise). Note how the PSNR values are close to the ones obtained using the real blur values.

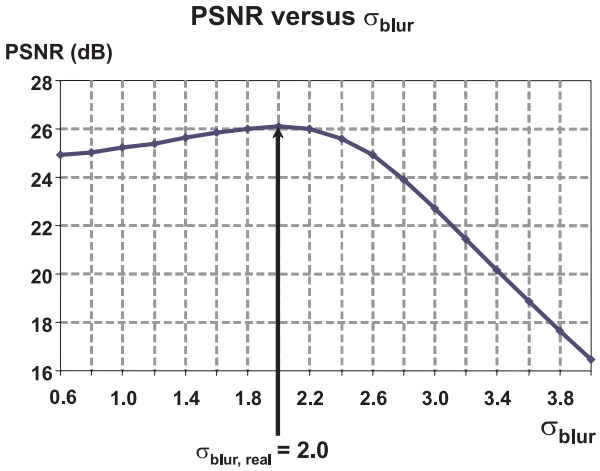

Figure 4. An example of the PSNR as a function of σ_{blur}. We artificially degraded the *Lake* image with $\sigma_{blur,real} = 2.0$ and $\sigma_{noise} = 10.0$. Then, the image was deconvolved with the Wiener filter using a range of candidate PSF's for which σ_{blur} was swept between 0.6 and 4.0 with stepsize 0.2 (but using the real value for σ_{noise}). For each candidate σ_{blur}, the PSNR of the restoration result was computed.

4. CONCLUSION

We have used a simple and robust criterion for estimating a single-parameter PSF function from a single observation of a degraded image. Using the kurtosis of a set of selected subbands as the criterion to be maximized, we have obtained satisfactory results for several examples of natural images and for a wide range of blur and noise levels. The method is robust, provides a reasonably small variance, and a very small bias (in contrast with previous methods (e.g., [17]). As a by-product, this method provides a semi-blind Wiener estimation of the original image, which, obviously, could be greatly improved by using the estimated PSF with a more powerful restoration method.

REFERENCES

1. S. I. Olsen, "Estimation of noise in images: An evaluation," *CVGIP: Graphical Models and Image Processing* **55**, pp. 319–323, July 1993.
2. D. Donoho and I. Johnstone, "De-noising by soft-thresholding," *IEEE Trans. Information Theory* **41**, pp. 613–627, May 1995.
3. D. Kundur and D. Hatzinakos, "Blind image deconvolution," *IEEE Signal Processing Magazine* **13**, pp. 43–64, May 1996.
4. D. Kundur and D. Hatzinakos, "Blind image deconvolution revisited," *IEEE Signal Processing Magazine* **13**, pp. 61–63, November 1996.
5. G. Ayers and J. Dainty, "Iterative blid deconvolution method and its applications," *Optics Letters* **13**, pp. 547–549, July 1988.
6. J. Seldin and J. Fienup, "Iterative blind deconvolution algorithm applied to phase retrieval," *Journal of the Optical Society of America A* **7**, pp. 428–433, March 1990.
7. T. Holmes, "Blind deconvolution of quantum limited incoherent imagery: maximum likelihood approach," *Journal of the Optical Society of America A* **9**, pp. 1052–1061, July 2000.
8. D. Fish, A. Brinicombe, and E. Pike, "Blind deconvolution by means of the richardson-lucy algorithm," *Journal of the Optical Society of America A* **12**, pp. 58–65, January 1995.
9. J. Flusser and T. Suk, "Degraded image analysis, an invariant approach," *IEEE Trans. Pattern Analysis and Machine Intelligence* **20**, pp. 1–14, June 1998.

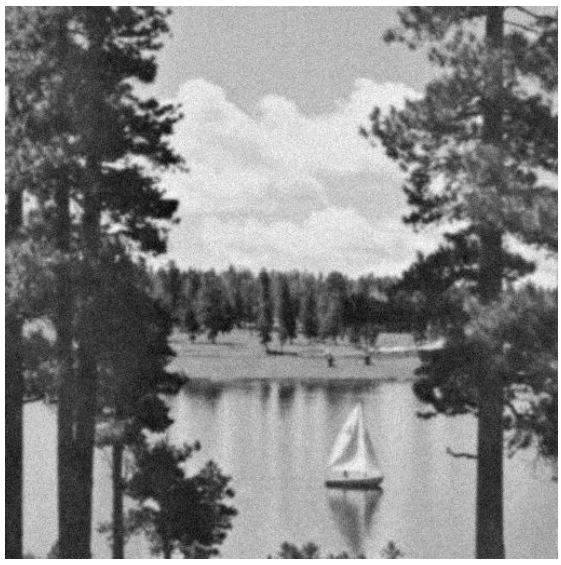

(a) Degraded image ($\sigma_{blur,real} = 1.0$, $\sigma_{noise} = 10$)
PSNR = 25.9dB

(b) Degraded image($\sigma_{blur,real} = 4.0$, $\sigma_{noise} = 0.1$)
PSNR = 22.0dB

(c) Restored image
with $\sigma_{blur,est} = 1.2$ PSNR = 28.7dB
with $\sigma_{blur,real}$ PSNR= 28.9dB

(d) Restored image
with $\sigma_{blur,est} = 4.1$ PSNR= 25.2dB
with $\sigma_{blur,real}$ PSNR= 25.3dB

Figure 5. Some examples of semi-blind Wiener restoration. The top row shows some degraded image examples, the bottom row as restored with our PSF estimation. The PSNR values (dB) are given for both our restoration and the restoration using the real blur.

10. D. Gennery, "Determination of optical transfer function by inspection of frequency domain plot," *Journal of the Optical Society of America* **63**, pp. 1571–1577, December 1973.
11. M. Cannon, "Blind deconvolution of spatially invariant image blurs with phase," *IEEE Trans. on Acoustics, Speech and Signal Processing* **ASSP-24**, pp. 58–63, February 2000.
12. M. Chang, A. Murat Tekalp, and A. Tanju Erdem, "Blur identification using the bispectrum," *IEEE Trans. Signal Processing* **39**, p. 2323, October 1991.

13. R. L. Lagendijk and J. Biemond, *Iterative Identification and Restoration of Images*, Kluwer Academic Publishers, Boston, Dordrecht, London, 1991.
14. G. Pavlović and A. Tekalp, "Maximum likelihood parametric blur identification based on a continouos spatial domain model," *IEEE Trans. Image Processing* **1**, pp. 496–504, October 1992.
15. S. Reeves and R. Mersereau, "Blur identification by the method of generalized cross-validation," *IEEE Trans. on Image Processing* **1**, pp. 301–311, July 1992.
16. S. Chardon, B. Vozel, and K. Chehdi, "Parametric blur estimation using the generalized cross-validation criterion and a smoothness constraint on the image," *Multidimensional Systems and Signal Processing* **10**, pp. 395–414, October 1999.
17. A. Savakis and H. J. Trussell, "Blur identification by residual spectral matching," *IEEE Trans. Image Processing* **2**, pp. 141–151, April 1993.
18. P. Comon, "Independent component analysis, a new concept?," *Signal Processing* **36**, pp. 287–314, April 1994.
19. J.-F. Cardoso and B. Laheld, "Equivariant adaptive source separation," *IEEE Trans. Signal Processing* **44**(12), pp. 3017–3030, 1996.
20. A. Bell and T. Sejnowsky, "The independent components of natural scenes are edge filters," *Vision Research* **37**(23), pp. 3201–3439, 1997.
21. A. Hyvärinen, "Sparse code shrinkage: Denoising of nongaussian data by maximum likelihood estimation," *Neural Computation* **11**, pp. 1739–1768, October 1999.
22. D. Field, "Relations between the statistics of natural images and the response properties of cortical cells," *Journal of the Optical Society of America A* **4**(12), pp. 2379–2394, 1987.
23. S. Mallat, "A theory for multiresolution signal decomposition," *IEEE Trans. Pattern Analysis and Machine Intelligence* **11**, pp. 674–693, July 1989.
24. B. Olshausen and D. Field, "Sparse coding with an overcomplete basis set: A strategy employed by v1?," *Vision Research* **37**, pp. 3311–3325, December 1997.